

Published in final edited form as:

Nature. 2007 October 18; 449(7164): 928–932. doi:10.1038/nature06160.

Arginine methylation at histone H3R2 controls deposition of H3K4 trimethylation

Antonis Kirmizis¹, Helena Santos-Rosa¹, Christopher J. Penkett², Michael A. Singer³, Michiel Vermeulen⁴, Matthias Mann⁴, Jürg Bähler², Roland D. Green³, and Tony Kouzarides¹

¹Gurdon Institute and Department of Pathology, Tennis Court Road, Cambridge CB2 1QN, UK

²Wellcome Trust Sanger Institute, Hinxton, Cambridge CB10 1HH, UK

³NimbleGen Systems, Inc., 1 Science Court, Madison, Wisconsin 53711, USA

⁴Max-Planck-Institute for Biochemistry, Department of Proteomics and Signal Transduction, Martinsried, Germany

Abstract

Modifications on histones control important biological processes through their effects on chromatin structure¹⁻³. Methylation at histone H3 lysine 4 (H3K4) is found at the 5' end of active genes and contributes to transcriptional activation by recruiting chromatin remodeling enzymes^{4,5}. An adjacent arginine residue (H3R2) is also known to be asymmetrically dimethylated (H3R2me2a) in mammalian cells⁶, but its location within genes and its function in transcription are unknown. Here we show that H3R2 is also methylated in budding yeast and using an antibody specific for H3R2me2a in ChIP-on-Chip analysis we determine the distribution of this modification on the entire yeast genome. We find that H3R2me2a is enriched throughout all heterochromatic loci and inactive euchromatic genes and is present at the 3'-end of moderately transcribed genes. In all cases the pattern of H3R2 methylation is mutually exclusive with the trimethyl form of H3K4 (H3K4me3). We show that methylation at H3R2 abrogates trimethylation of H3K4 by the Set1 methyltransferase. The specific effect on H3K4me3 results from the occlusion of Spp1, a Set1-methyltransferase subunit necessary for trimethylation. Thus, the inability of Spp1 to recognise H3 methylated at R2 prevents Set1 from trimethylating H3K4. These results provide the first mechanistic insight into the function of arginine methylation on chromatin.

Methylation at lysine and arginine residues within histones has been linked to gene expression¹⁻³. Studies in mammalian cells have demonstrated that histone arginine methylation can influence both gene activation and repression. However, the precise mechanism employed by arginine methylation to exert its effects on the chromatin template remains elusive. In contrast, increasing evidence shows that lysine methylation modulates gene expression by recruiting downstream effector proteins. Recent findings showed that methylation at H3K4 (H3K4me) controls transcription activation by recruiting chromatin remodeling activities^{4,5}. This recruitment can be specific for the ^{7,8} trimethyl form of H3K4 (H3K4me3) indicating that the three different methyl states of H3K4 (mono-, di-, or tri-)

Correspondence and requests for materials should be addressed to T.K. (t.kouzarides@gurdon.cam.ac.uk).

Supplementary Information accompanies the paper on www.nature.com/nature.

Author Information The microarray data sets are available from GEO (Gene Expression Omnibus) under accession number GSE8626, and from <http://www.gurdon.cam.ac.uk/%7Ekouzarideslab/H3R2methylation.html>.

The authors declare competing financial interests.

play distinct roles in gene expression. The set1 complex is the enzyme that can mediate methylation of H3K4 and various components of the complex regulate the establishment of the different methyl-H3K4 states⁹⁻¹¹

To investigate the role of methylation at histone H3 arginine 2 (H3R2) in gene expression we raised an antibody against the asymmetric dimethylated form of H3R2 (H3R2me2a). This modification is known to be catalysed by the mammalian CARM1/PRMT4 *in vitro*¹² and is affected by deletion of this methyltransferase in mouse embryonic fibroblasts⁶. Immunoblot analysis reveals that H3R2me2a is present *in vivo*, on mammalian and yeast histone H3 (Supplementary Fig. S1A and S1B). We confirmed the specificity of this antibody towards H3R2me2a by dot-blot analysis and peptide competition assays (Supplementary Fig. S1C and S1D). Most importantly, the antibody does not recognize histone H3 in yeast cells where arginine 2 is mutated to an alanine (H3R2A), a glutamine (H3R2Q), or a lysine (H3R2K) (Supplementary Fig. S1E and S2).

In an attempt to understand the specific function of H3R2 methylation, we used a high-resolution ChIP-on-chip analysis in yeast to determine its genome-wide distribution. We found that this mark is associated with both heterochromatin and euchromatin (Fig. 1 and 2). Analysis of heterochromatin showed that H3R2me2a is present at all four heterochromatic regions in yeast: the two silent mating type loci (*HMR* and *HML*), the rRNA-encoding DNA (*rDNA* repeat), and telomeres (Fig. 1a-d). In this analysis it became clear that all heterochromatic regions that were enriched in H3R2 methylation were also devoid of the active methyl-mark H3K4me3 (Fig. 1a-d). Indeed the drop in H3R2me2a and rise in H3K4me3 levels can be used to define the boundaries of heterochromatic regions.

The presence of H3R2me2a at heterochromatic sites suggest that this methylation may be part of a signal to silence transcription. We therefore used yeast strains expressing H3R2 mutants, H3R2A and H3R2Q, to test the role of this residue in heterochromatic silencing. We found that mutation of arginine 2 resulted in severe loss of silencing at the *HMR*, telomere, and *rDNA*, and to a moderate extent at the *HML* locus (Fig. 1e and Supplementary Fig. S3, left panels). These results indicate that arginine 2 on H3 is necessary for heterochromatic silencing suggesting a role for H3R2 methylation in this process.

We next considered the mechanism by which H3R2me2a may function to regulate heterochromatin. Comparison of the occupancy of key heterochromatic factors, such as Rap1p and Sir2p, with H3R2me2a enrichment indicates a coincidence at telomeric sites (compare Fig. 1d to 1f). However, when ChIP analysis of Rap1p and Sir2p was compared in WT and H3R2A strains the binding levels of these two proteins at the heterochromatic sites was not changed (Fig. 1f). These results indicate that methylation at H3R2 functions at heterochromatin through a novel mechanism, which is independent of Rap1p and Sir2p recruitment. However, we cannot exclude the possibility that disruption of H3K4 methylation may contribute to the H3R2A phenotype (see below).

In order to determine the role of H3R2me2a within euchromatin, we divided 5065 genes into five groups according to their transcriptional rate¹³ (designated by shades of blue in Fig. 2a). We then examined the average enrichment of H3R2me2a for each gene group. Composite profiles indicate that H3R2me2a occurs near the middle of the coding region and peaks towards the 3' end of genes (Fig. 2a). The H3R2me2a enrichment inversely correlates with transcriptional activity since this mark is most abundant on the least active genes.

A role for H3R2 methylation in transcriptional repression was also highlighted by comparing its genomic profile to the pattern of trimethyl-H3K4, which is a signal for active transcription. Figure 2b shows that H3K4me3 is found at the 5' end of genes, consistent with previous studies^{14,15}, and that it is most enriched at the most active genes (darker shades of

blue). We noticed that H3K4me3 is enriched in the region of a gene where H3R2me2a is missing, suggesting an antagonistic relationship between these two modifications (Fig. 2a and 2b).

To investigate the relationship of H3R2me2a with all H3K4 methyl states we divided all genes into three transcriptional categories (inactive, moderately transcribed, and highly transcribed) and then compared the distribution of H3R2me2a with that of the three methyl-H3K4 marks (H3K4me1, H3K4me2, and H3K4me3) across individual genes. In all three transcriptional states the pattern of H3R2me2a is mutually exclusive specifically with H3K4me3 (Fig. 2c-e and Supplementary Fig. S4). This inverse enrichment between H3R2me2a and H3K4me3 is not seen with trimethylation of the other two known modified lysines in yeast, H3K36me3 and H3K79me3 (data not shown). Importantly, the inverse profiles of H3R2me2a and H3K4me3 are not due to failure of the anti-H3R2me2a and anti-H3K4me3 antibodies to recognize their epitope when the adjacent residue is methylated (Supplementary Fig. S1C). These results indicate that H3R2me2a covers the promoter and coding region of silent genes but, as the transcription rate is increased, H3R2me2a recedes from the 5'-end and is replaced by H3K4 trimethylation.

We next asked whether H3R2me2a and H3K4me3 are dynamically exchanged on nucleosomes upon induction of gene expression. ChIP analysis of cells grown in repressive conditions (glucose) showed high enrichment of H3R2me2a at *GAL* genes, while H3K4me3 was not detected at all on the same loci (Fig. 2f, grey bars). Most significantly, shifting the cells to activating conditions (galactose) completely reversed the levels of the two modifications at those same locations (Fig. 2f, black bars). This analysis confirms the inverse correlation observed between H3R2me2a and H3K4me3, and demonstrates that the two modifications are dynamically co-regulated in the sense that when one mark is removed from nucleosomes the other one is incorporated.

The dynamic exchange of these two modifications on nucleosomes suggested that the arginine at position 2 of histone H3 might play a direct role in regulating the methylation at the adjacent lysine 4. We examined this possibility by analysing the global methylation levels at H3K4 in yeast strains carrying mutations in H3R2 (H3R2A, H3R2Q, and H3R2K). Figure 3a and supplementary figure S2 show that in the H3R2A and H3R2Q strains the H3K4me3 signal is abolished while in the H3R2K strain the trimethyl-H3K4 signal is greatly reduced. The H3K4me1 and H3K4me2 are, respectively, unaffected or very slightly reduced in these mutant strains (Fig. 3a, lane 3 and Supplementary Fig. S2, lanes 2-4). The disruption of H3K4me3 by mutating H3R2 is specific, as the H3R2A mutation does not affect the trimethyl state at the other methylated sites, H3K36 and H3K79 (Fig. 3a, lane 3). Importantly, the loss of the trimethyl-H3K4 signal in the H3R2A mutant is not due to failure of the anti-H3K4me3 antibody to recognize its epitope when arginine 2 is mutated (Supplementary Fig. S5 lane 3, left and right panels).

The fact that trimethylation of H3K4 defines active transcription¹⁶ prompted us to ask if the H3R2A mutation affected gene expression. We tested the kinetics of *GAL1* and *GAL7* induction in WT, H3R2A and H3K4A mutant strains. Figure 3b demonstrates that mutation of H3R2 delays the activation of *GAL* genes. The effect of the H3R2A mutation is similar, but less severe, to that of the H3K4A mutation indicating that these two residues might be involved in a common regulatory mechanism (Fig. 3b).

We next sought to determine the mechanism responsible for the inverse distribution between dimethyl-H3R2 and trimethyl-H3K4. We first considered the possibility that H3R2 forms part of the recognition site for the Set1-complex, which methylates H3K4. Figure 3c shows that yeast purified Set1-complex is able to methylate an unmodified H3 peptide but its

activity is inhibited by mutation of arginine 2 to alanine (compare lane 2 with lane 4). Importantly, asymmetric dimethylation at H3R2 also inhibits Set1-complex activity towards lysine 4 (Fig. 3c, compare lanes 1 and 2). This Set1p activity is specific for lysine 4, since a peptide that is already trimethylated at H3K4 shows only background signal (Fig. 3c, lane 3). In addition, peptide sequencing reveals that the activity of Set1-complex is occurring only at residue 4 (Supplementary Fig. S6). These results suggest that (a) H3R2 is a recognition site for the Set1p methylase complex and that (b) methylation of H3R2 inhibits the Set1p enzyme from methylating H3K4.

The ability of Set1p to catalyze mono-, di-, or tri-methylation at H3K4 is regulated by a number of Set1-complex components. Specifically, the Spp1 subunit is required for Set1-mediated trimethylation of H3K4¹⁰. Recently, it has been shown that Spp1 binds specifically to di- and tri-methyl H3K4 via its PHD domain¹⁷. We therefore asked whether methylation of H3R2 is required for the binding of Spp1 to methylated lysine 4 *in vitro*. Figure 4a shows that di-methylation of H3R2 inhibits the interaction of the Spp1 PHD-finger with di- or trimethylated K4 (compare lanes 3 and 5 with lanes 4 and 6). Mutation of H3R2 also disrupts the binding of Spp1, consistent with the fact that this arginine residue is part of the recognition site of the Spp1 PHD finger¹⁷ (Supplementary Fig. S7). To determine whether H3R2me2a also blocks Spp1 binding *in vivo* we performed ChIP assays in a yeast strain expressing myc-tagged Spp1. Figure 4b and supplementary figure S8 show that Spp1 is bound to regions of genes that were trimethylated at H3K4 and were devoid of H3R2me2a. However, Spp1 was absent in areas of genes where H3R2 methylation was present even though H3K4me1 or H3K4me2 were also abundant in these regions (Fig. 4b, middle panel and Supplementary Fig. S8). These results confirm the biochemical analysis in figure 4a which shows that H3R2 methylation can prevent Spp1 from binding di-methylated H3K4. Consistent with this occlusion of Spp1, no trimethylation of H3K4 is seen in the region of genes where H3R2me2a is found.

Together these results identify the existence and point to a function of H3R2 methylation in yeast. H3R2 methylation regulates the activity of the Set1-complex towards H3K4 by modulating the binding of its Spp1 component. The role of H3R2me2a in controlling H3K4me3 is also conserved in humans¹⁸ suggesting that this mechanism will be generally applicable in all eukaryotes.

These findings place methylation at H3R2 and H3K4 in the same pathway and support a role of dimethyl-H3R2 as a negative regulator of H3K4 trimethylation. Figure 4c shows a model of how H3R2me2a may function during the transition from a repressed to a transcriptionally active state on a gene. Global analysis shows that when a gene is inactive, H3R2me2a is present throughout the promoter and coding region (step 0). Methylation of H3R2 in yeast is likely to be catalyzed by a novel, yet to be identified methyltransferase, as combinatorial deletion of the three known arginine methyltransferases (Rmt1, Rmt2, and Hsl7) does not affect the levels of this modification (data not shown). At this silent stage (step 0) very little if any methylation of H3K4 takes place. During activation, the presence of methylated H3R2 does not inhibit Set1p from mono- or di-methylating H3K4 (step 1). However, in order for trimethylation of H3K4 to take place, methylation at H3R2 has to be removed (step 2). The clearing of methylation at H3R2 must be mediated either by histone replacement or the action of an as yet to be identified arginine demethylase. Once a region becomes devoid of H3R2 methylation, the Spp1 protein can recognise H3K4me2 via its PHD domain. This binding probably extends the time of interaction between Set1-complex and its substrate thus, promoting trimethylation of H3K4 by Set1p (step 3, ¹⁹). Spp1 then associates with H3K4me3 (step 4), possibly to protect this methyl state from the action of the trimethyl-H3K4 demethylase Jhd2^{20,21}. At the same time, Spp1 may protect H3R2 from methylation since structural studies^{17,22,23} show that this arginine residue is absolutely required for the

association of the Spp1 PHD finger with methylated H3K4. Together these data indicate that arginine methylation at H3R2 may influence transcription by regulating the H3K4 trimethylation capacity of the Set1 methyltransferase.

Methods

ChIP-on-chip

Formaldehyde cross-linking and chromatin immunoprecipitations (ChIP) were performed as described before²⁴ with the following exceptions: the immunocomplexes were eluted from the Sepharose beads (Amersham) using a total of 200 ul elution buffer (100 mM Sodium bicarbonate, 1% SDS) and RNase (Roche) treatment was performed during reversing of the cross-links at 65°C for 5 hours. After reversing the cross-links, each individual ChIP sample was purified using the Qiaquick PCR purification kit (QIAGEN) and DNA was eluted from the columns with 50 ul of EB buffer. Amplicons were generated from individual ChIP samples using a Linker-Mediated PCR. Sample labeling, hybridization, and data extraction were performed by NimbleGen Systems Inc as part of a ChIP Array Service. Downstream analysis of the ChIP-on-chip data was performed with the statistical package R (www.R-project.org) and associated array analysis modules in Bioconductor.

Details of additional methods used in this study are included in Supplementary Information.

Supplementary Material

Refer to Web version on PubMed Central for supplementary material.

Acknowledgments

We thank Chris Nelson, Andy Bannister, and Maria Christophorou for critical reading of the manuscript; Samuel Marguerat for helpful discussions; Len Packman, and Mike Weldon for assistance with protein sequencing; Nan Jiang and Rebecca Selzer for assistance with microarray analyses; and Mike Gilchrist for help with displaying genomic data. This work was supported by postdoctoral fellowship grants to A.K. from the European Molecular Biology Organization (EMBO) and Marie Curie. The T.K. lab is funded by grants from Cancer Research UK (CRUK) and the European Community (Eupitron).

References

1. Kouzarides T. Chromatin modifications and their function. *Cell*. 2007; 128:693–705. [PubMed: 17320507]
2. Martin C, Zhang Y. The diverse functions of histone lysine methylation. *Nat Rev Mol Cell Biol*. 2005; 6:838–49. [PubMed: 16261189]
3. Wysocka J, Allis CD, Coonrod S. Histone arginine methylation and its dynamic regulation. *Front Biosci*. 2006; 11:344–55. [PubMed: 16146736]
4. Ruthenburg AJ, Allis CD, Wysocka J. Methylation of lysine 4 on histone H3: intricacy of writing and reading a single epigenetic mark. *Mol Cell*. 2007; 25:15–30. [PubMed: 17218268]
5. Sims RJ 3rd, Reinberg D. Histone H3 Lys 4 methylation: caught in a bind? *Genes Dev*. 2006; 20:2779–86. [PubMed: 17043307]
6. Torres-Padilla ME, Parfitt DE, Kouzarides T, Zernicka-Goetz M. Histone arginine methylation regulates pluripotency in the early mouse embryo. *Nature*. 2007; 445:214–8. [PubMed: 17215844]
7. Shi X, et al. ING2 PHD domain links histone H3 lysine 4 methylation to active gene repression. *Nature*. 2006; 442:96–9. [PubMed: 16728974]
8. Wysocka J, et al. A PHD finger of NURF couples histone H3 lysine 4 trimethylation with chromatin remodelling. *Nature*. 2006; 442:86–90. [PubMed: 16728976]
9. Dou Y, et al. Regulation of MLL1 H3K4 methyltransferase activity by its core components. *Nat Struct Mol Biol*. 2006; 13:713–9. [PubMed: 16878130]

10. Schneider J, et al. Molecular regulation of histone H3 trimethylation by COMPASS and the regulation of gene expression. *Mol Cell*. 2005; 19:849–56. [PubMed: 16168379]
11. Steward MM, et al. Molecular regulation of H3K4 trimethylation by ASH2L, a shared subunit of MLL complexes. *Nat Struct Mol Biol*. 2006; 13:852–4. [PubMed: 16892064]
12. Schurter BT, et al. Methylation of histone H3 by coactivator-associated arginine methyltransferase 1. *Biochemistry*. 2001; 40:5747–56. [PubMed: 11341840]
13. Holstege FC, et al. Dissecting the regulatory circuitry of a eukaryotic genome. *Cell*. 1998; 95:717–28. [PubMed: 9845373]
14. Liu CL, et al. Single-nucleosome mapping of histone modifications in *S. cerevisiae*. *PLoS Biol*. 2005; 3:e328. [PubMed: 16122352]
15. Pokholok DK, et al. Genome-wide map of nucleosome acetylation and methylation in yeast. *Cell*. 2005; 122:517–27. [PubMed: 16122420]
16. Santos-Rosa H, et al. Active genes are tri-methylated at K4 of histone H3. *Nature*. 2002; 419:407–411. [PubMed: 12353038]
17. Shi X, et al. Proteome-wide analysis in *Saccharomyces cerevisiae* identifies several PHD fingers as novel direct and selective binding modules of histone H3 methylated at either lysine 4 or lysine 36. *J Biol Chem*. 2007; 282:2450–5. [PubMed: 17142463]
18. Guccione E, et al. Methylation of histone H3R2 by PRMT6 and H3K4 by an MLL complex are mutually exclusive. *Nature*. 2007 in press.
19. Wood A, et al. Ctk complex-mediated regulation of histone methylation by COMPASS. *Mol Cell Biol*. 2007; 27:709–20. [PubMed: 17088385]
20. Liang G, Klose RJ, Gardner KE, Zhang Y. Yeast Jhd2p is a histone H3 Lys4 trimethyl demethylase. *Nat Struct Mol Biol*. 2007; 14:243–245. [PubMed: 17310254]
21. Seward DJ, et al. Demethylation of trimethylated histone H3 Lys4 in vivo by JARID1 JmjC proteins. *Nat Struct Mol Biol*. 2007; 14:240–2. [PubMed: 17310255]
22. Li H, et al. Molecular basis for site-specific read-out of histone H3K4me3 by the BPTF PHD finger of NURF. *Nature*. 2006; 442:91–5. [PubMed: 16728978]
23. Pena PV, et al. Molecular mechanism of histone H3K4me3 recognition by plant homeodomain of ING2. *Nature*. 2006; 442:100–3. [PubMed: 16728977]
24. Morillon A, O'Sullivan J, Azad A, Proudfoot N, Mellor J. Regulation of elongating RNA polymerase II by forkhead transcription factors in yeast. *Science*. 2003; 300:492–5. [PubMed: 12702877]

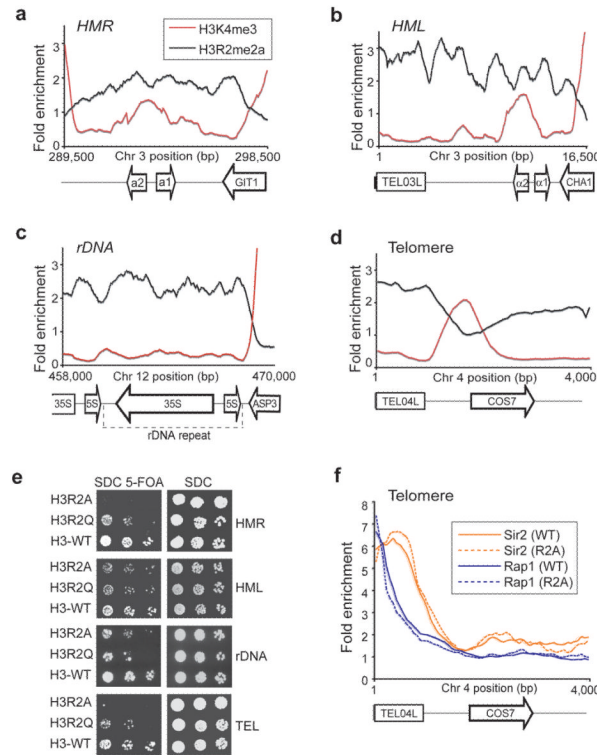


Figure 1. H3R2me2a associates with heterochromatin

(a-d) ChIP-on-chip analysis was performed in wild-type yeast cells (BY4741) grown to mid-log phase using antibodies to H3R2me2a and H3K4me3. The graphs show a moving average (window=15, step=1) of the H3R2me2a and H3K4me3 enrichment normalized to histone H3 occupancy at the right (*HMR*) and left mating type cassettes (*HML*), at the silent ribosomal DNA repeat region (*rDNA*) and at the left telomere of chromosome 4 (*TEL04L*). Values less than 1 represent regions that are not enriched. The arrows at the bottom of the graphs represent the location of genes and the direction they are transcribed. The rectangles at the bottom of the graphs correspond to the telomeric sequences. (e) Heterochromatin silencing assays were performed using cells from the H3R2A, H3R2Q, and isogenic wild-type (H3) yeast strains. Plates were photographed after 48 h incubation at 30 °C. (f) ChIP-on-chip analysis on telomeres using antibodies against Sir2p and Rap1p in WT and H3R2A strains. The graph shows a moving average (window=15, step=1) of the antibody enrichment as a ratio to Input at *TEL04L*.

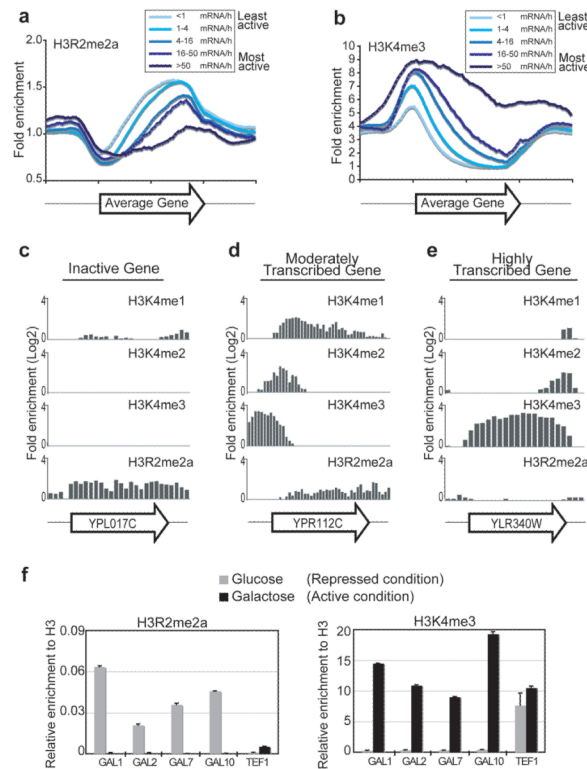


Figure 2. H3R2me2a enrichment at euchromatic genes is mutually exclusive to H3K4me3 (a and b) ChIP-on-chip analysis was performed in wild-type yeast cells (BY4741) grown to mid-log phase using the anti-H3R2me2a and anti-H3K4me3 antibodies. The graphs represent composite profiles of H3R2me2a and H3K4me3 at 5065 genes, which were divided into five groups according to their transcriptional rate¹². (c-e) ChIP-on-chip analysis was performed as above using antibodies to H3K4me1, H3K4me2, H3K4me3, and H3R2me2a. The distribution of these modifications is compared at three differentially expressed genes. The name of each gene (arrow) is shown at the bottom of the graphs. (f) ChIP experiments were performed in yeast cells grown in either glucose (grey bars) or galactose as carbon source (black bars) using antibodies to H3R2me2a (left panel) and H3K4me3 (right panel). The precipitated DNA was analyzed by quantitative PCR using primers specific to the indicated genes. Standard errors were calculated for duplicate experiments. The induction of gene expression from glucose to galactose containing medium was monitored by RT-PCR analysis (see Supplementary Fig. S9).

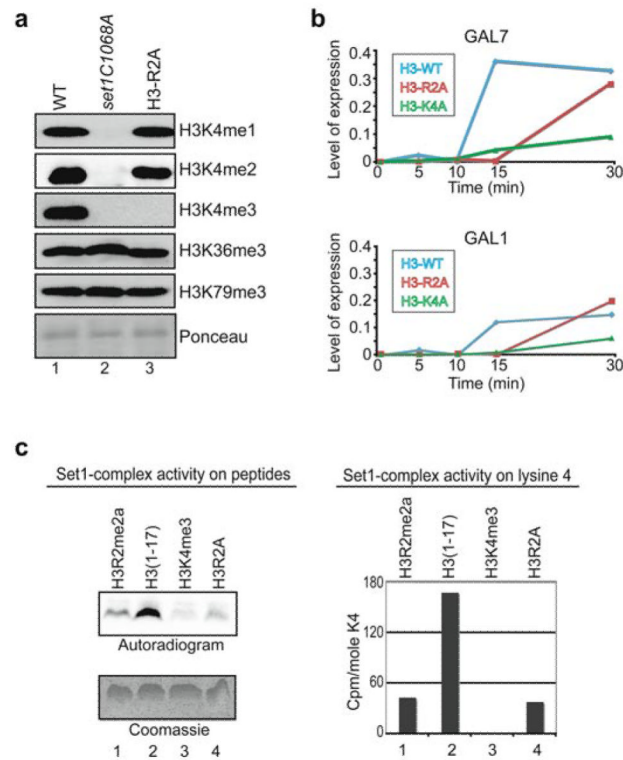


Figure 3. H3R2me2a regulates the Set1-complex activity towards H3K4

(a) Whole yeast extracts prepared from the H3R2A (lane 3), *set1C1068A* (lane 2), and isogenic WT (lane 1) strains were analyzed by Western blotting using antibodies to H3K4me1, H3K4me2, H3K4me3, H3K36me3, or H3K79me3. Uniform loading was monitored by Ponceau stain. (b) Yeast cells expressing wild-type, R2A mutant, or K4A mutant histone H3 were grown to mid-log phase in media containing raffinose (inactive condition) and then shifted to media containing galactose (activating condition). RNA was prepared at the indicated times and analyzed by quantitative RT-PCR using primers specific to *GAL7* (top panel) and *GAL1* (bottom panel). Values show the expression of *GAL7* or *GAL1* normalized to the RNA levels of *RTG2* whose expression remains unchanged. The experiment was repeated with similar results. (c) Yeast purified Set1-complex was incubated with 3H-SAM in the presence of an asymmetrically dimethylated H3R2 peptide (aa 1–17, lane 1), an unmodified peptide (aa 1–17, lane 2), a trimethylated H3K4 peptide (aa 1–17, lane 3), or an H3R2A mutant peptide (aa 1–17, lane 4). Peptides were analyzed for radioactive labelling using autoradiography (left panel) or sequential Edman degradation (right panel). Equal loading of peptides was monitored by Coomassie stain (left panel). The radioactivity released at lysine 4 of the H3K4me3 peptide (lane 3) was regarded as background signal and was subtracted from the lysine 4 signals of the other three peptides (right panel). The methylase assay was repeated three times with similar results.

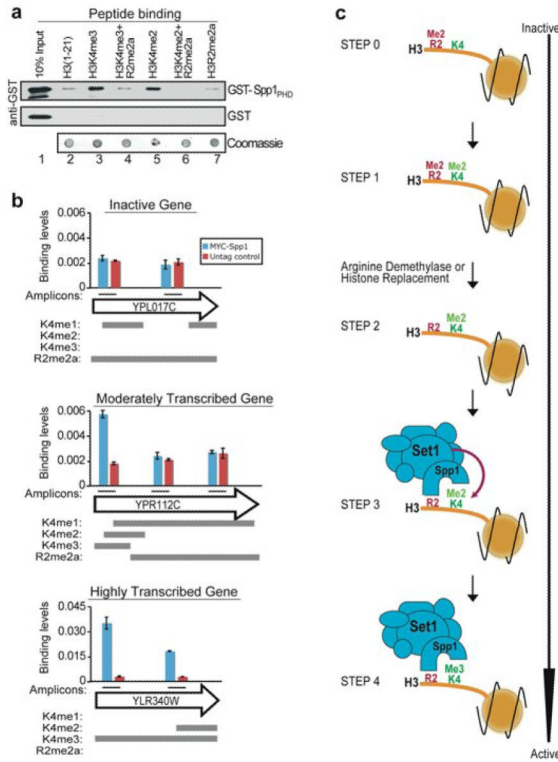


Figure 4. H3R2me2a blocks the binding of Spp1 to methylated H3K4

(a) *In vitro* binding assays were performed using synthetic histone H3 N-terminal peptides (aa 1-21) and either recombinant GST-Spp1PHD (top panel) or GST alone (middle panel). The bound proteins were monitored by western analysis using a GST antibody. Peptide coupling was controlled by dot-blotting followed by Coomassie staining (bottom panel). (b) *In vivo* binding analysis of Spp1 was performed using ChIP assays followed by quantitative PCR. Chromatin from yeast cells expressing a tagged (Myc-Spp1) or an untagged (Control) form of Spp1 was immunoprecipitated with anti-Myc antibody. The analysed amplicons within each gene (arrow) are indicated by black lines. Standard errors were calculated for duplicate experiments. The grey bars below each plot show the distribution of mono-, di-, tri-H3K4 and H3R2me2a within each gene. (c) Model of how methylation at histone H3R2 controls trimethylation at H3K4.